

# Scientific synthetic report - project IDEI-0153 (2011-2016): 'ADVANCED STUDIES ON STRUCTURE AND DYNAMICS OF EXOTIC NUCLEI'

## I. Coexistence phenomena in exotic neutron-rich $A \sim 100$ nuclei within beyond-mean-field approach

### I. 1. Shape coexistence in the $N=58$ Sr and Zr nuclei

The structure of neutron-rich nuclei in the  $A \sim 100$  mass region relevant for the r-process as well as reactor decay heat manifests drastic changes in some isotopic chains and often sudden variations of particular nuclear properties have been identified.

Neutron-rich Sr and Zr nuclei indicate rapid transition from spherical to deformed shape with a possible identification of the sudden onset of quadrupole deformation increasing the neutron number from  $N = 58$  to  $N = 60$ . The structure and dynamics of  $^{96}\text{Sr}$  and  $^{98}\text{Zr}$  have been investigated in the frame of the *complex* Excited Vampir (EXVAM) beyond-mean-field approach using a large model space and a realistic effective two-body interaction.

Intense studies based on *complex* Monster (Vampir) model have been dedicated to the renormalisation of the effective two-body interaction in a large model space, including above the  $^{40}\text{Ca}$  core  $1p_{1/2}$ ,  $1p_{3/2}$ ,  $0f_{5/2}$ ,  $0f_{7/2}$ ,  $2s_{1/2}$ ,  $1d_{3/2}$ ,  $1d_{5/2}$ ,  $0g_{7/2}$ ,  $0g_{9/2}$ , and  $0h_{11/2}$  oscillator orbits for both protons and neutrons in the valence space.

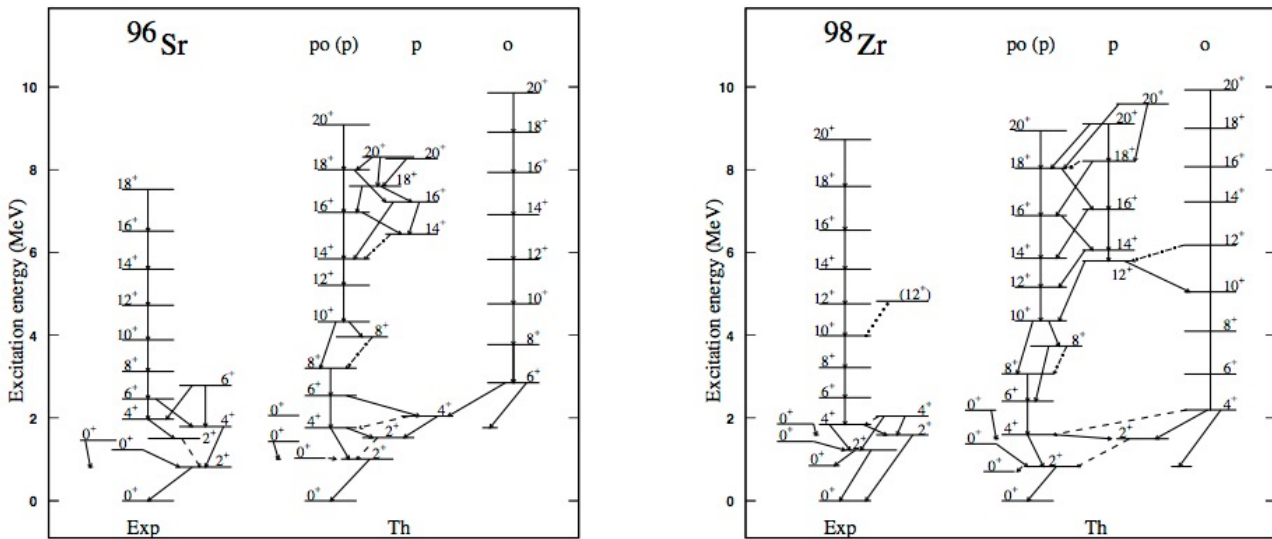


Fig.1 Theoretical EXVAM spectrum of  $^{96}\text{Sr}$  (left) and  $^{98}\text{Zr}$  (right) compared to experimental data [1].

The effective two-body interaction is constructed from a nuclear matter  $G$  matrix based on the Bonn  $A$  potential. In order to enhance the pairing properties the  $G$  matrix was modified by three short-range Gaussians in the  $T=1$  and  $T=0$  channel. In addition the isoscalar interaction was modified by monopole shifts for all  $T=0$  matrix elements of the form  $\langle 0g_{9/2}0f_{IT=0} | G | 0g_{9/2}0f_{IT=0} \rangle$  involving protons and neutrons occupying the  $0f_{5/2}$  and the  $0f_{7/2}$  orbitals. The Coulomb interaction between the valence protons was added [1].

We studied the lowest positive-parity states up to spin  $20^+$  in  $^{96}\text{Sr}$  and  $^{98}\text{Zr}$  [1]. For each nucleus the calculated states have been organized in bands based on the  $B(E2; \Delta I = 2)$  values connecting them. The theoretical lowest bands of  $^{96}\text{Sr}$  and  $^{98}\text{Zr}$  are compared to the experimental data in Figure 1.

Table I: Structure of wave functions for  $0^+$  states

$I[\hbar]$	$^{96}\text{Sr}$			$^{98}\text{Zr}$		
	spherical	prolate	oblate	spherical	prolate	oblate
$0_1^+$	36%	20%	44%	12%	43%	45%
$0_2^+$	57%	18%	25%	84%	12%	4%
$0_3^+$		69%	31%	1%	57%	42%
$0_4^+$	4%	6%	90%	2%	10%	88%

The states building the  $po(p)$ -band in each nucleus are characterised by strong prolate-oblate mixing at low spins and variable prolate mixing at intermediate and high spins. At intermediate and high spins prolate and oblate bands coexist in both nuclei. A particular situation is found for the  $0^+$  states: the lowest projected EXVAM configuration is spherical in both nuclei. In  $^{96}\text{Sr}$  the second  $0^+$

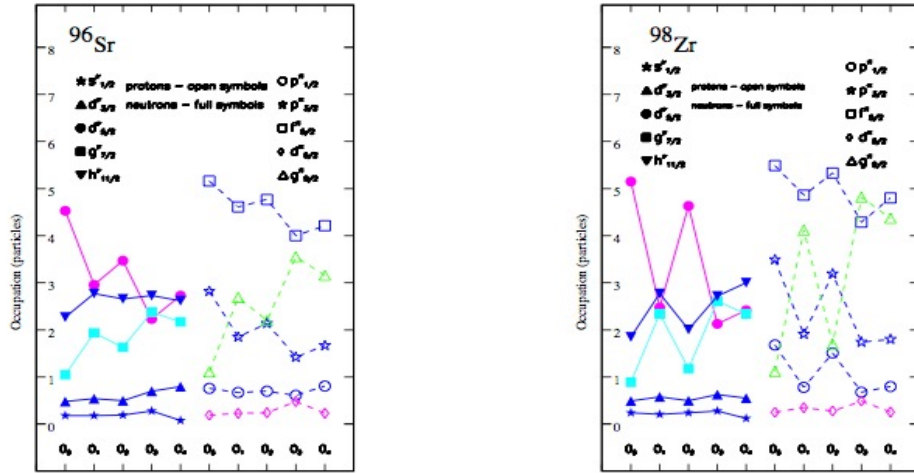


Fig.2 Occupation of valence spherical orbitals for  $0^+$  states in  $^{96}\text{Sr}$  (left) and  $^{98}\text{Zr}$  (right) [1]

configuration is oblate deformed in the intrinsic system, the third one is prolate. In  $^{98}\text{Zr}$  the second configuration is prolate, the third is oblate. The structure of the lowest four  $0^+$  states in terms of spherical, prolate, and oblate content is presented in Table I. Support for the mixing of configurations with different intrinsic deformations in the structure of the wave functions for the  $0^+$  states is offered by the strong  $\rho^2(E0)$  values found theoretically and experimentally in both nuclei. In Figure 2 we present the occupation of valence single-particle orbitals for the spherical  $0^+$

EXVAM configuration (the first state in the row for each nucleus) and for the lowest four  $0^+$  states in  $^{96}\text{Sr}$  and  $^{98}\text{Zr}$ , respectively.

The occupation of the  $1d_{5/2}$  neutron orbital is essential for the spherical  $0^+$  EXVAM configuration. The occupation of the  $0g_{9/2}$  proton orbital is significantly changing from the intrinsically oblate deformed configurations to the prolate deformed ones in both nuclei.

The evolution of the structural changes is correlated with the faster alignment of the neutrons with respect to the protons corroborated with the variation of theoretical gyromagnetic factors [2]. The variable configuration mixing of the wave functions is revealed in the evolution of the spectroscopic quadrupole moments and in- and inter-band  $B(E2)$  strengths [2,3]. Strong oblate-prolate mixing at low spins is supported by the recent experimental results on quadrupole moments and  $B(E2)$  strengths. The EXVAM scenarios for the triple shape coexistence: spherical, oblate and prolate specific for the  $0^+$  states is confirmed and used in the literature for the interpretation of the experimental results in the neighbouring nuclei.

## I. 2. Gamow-Teller beta decay of $^{102,104}\text{Tc}$

The Gamow-Teller (GT)  $\beta$  decay of neutron-rich  $A\sim 100$  nuclei is not only relevant to nuclear structure, but is of high interest in nuclear technology. The estimation and control of the heat emitted by the decay of fission products requires certain still missing useful information, such as a knowledge of the decay properties of specific nuclei that contribute to the heating of the reactor during and after operation. The Gamow-Teller strengths distributions and the accumulated strength for the decay of  $^{102}\text{Tc}$  to  $^{102}\text{Ru}$  and  $^{104}\text{Tc}$  to  $^{104}\text{Ru}$  are self-consistently investigated for the first time in the frame of *complex* Excited Vampir model in a large model space using a realistic two-body interaction.

We investigated the lowest  $1^+$  states in  $^{102}\text{Tc}$ , the lowest  $3^+$  states in  $^{104}\text{Tc}$ , and the positive-parity states up to spin  $4^+$  in  $^{102}\text{Ru}$  and  $^{104}\text{Ru}$  [4]. The experimental data indicate 3 orders of magnitude difference in the  $\beta$ -decay half-life of the two Tc isotopes. The mixing of differently deformed configurations obtained self-consistently in the frame of *complex* Excited Vampir model, which dominate the structure of both even-even parent and odd-odd daughter nucleus, gives a scenario in good agreement with the experimental data obtained using Total Absorption Gamma Spectrometer

Table II: Spectroscopic quadrupole moments (in  $efm^2$ ) of  $^{102}\text{Ru}$  and  $^{104}\text{Ru}$  states

$^{102}\text{Ru}$	$^{104}\text{Ru}$	
$2^+$ -states	$2^+$ -states	$4^+$ -states
-19.2	-28.0	34.3
23.7	42.0	-17.0
-14.7	54.4	71.1
30.1	-44.0	-82.9
3.9	50.1	-7.6

(TAGS) [4]. The obtained results indicate that the structure of the wave function for the lowest  $1^+$

state of  $^{102}\text{Tc}$  manifests a strong mixing of differently deformed prolate and oblate configurations in the intrinsic system. Altogether the prolate components represent 53% of the total amplitude and the oblate components make 47% in the structure of the wave function while the wave function for the lowest  $3^+$  state of  $^{104}\text{Tc}$  is dominated (99%) by a single prolate deformed configuration. The wave functions of the daughter states with significant Gamow-Teller strength manifest significant oblate-prolate mixing and the corresponding spectroscopic quadrupole moments are presented in Table II [5].

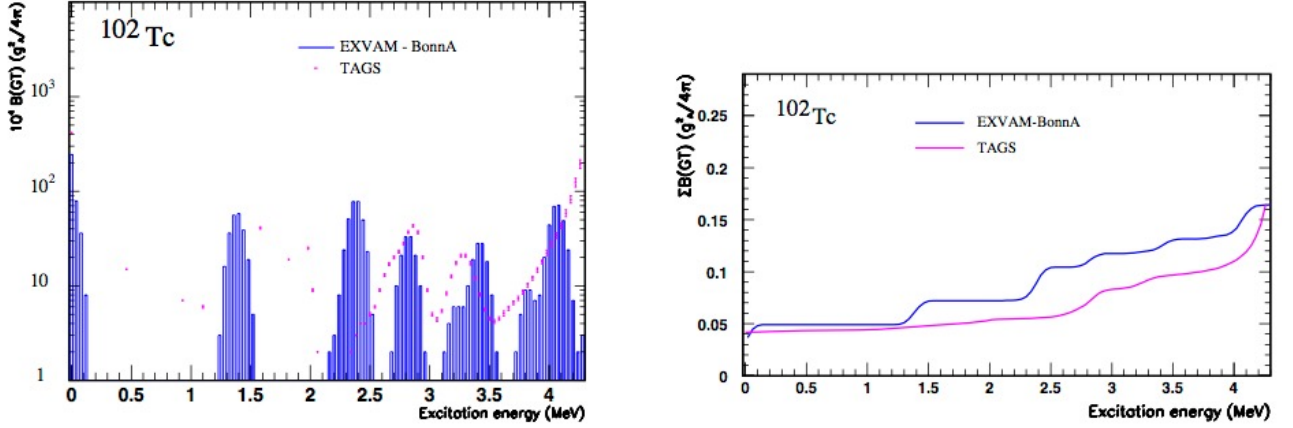


Fig.3: The Gamow-Teller strength distribution and the corresponding accumulated strength for  $^{102}\text{Tc}$  obtained within the *complex* Excited Vampir model compared with TAGS results[4,5].

The Gamow-Teller strength distribution and the corresponding accumulated Gamow-Teller strength for the decay of the  $1^+$  parent state in  $^{102}\text{Tc}$  to the calculated  $0^+$  and  $2^+$  daughter states in  $^{102}\text{Ru}$  is presented in Figure 3 compared with TAGS results. The GT strength for the decay to the  $1^+$  states in  $^{102}\text{Ru}$  is negligible. The Gamow-Teller strength distribution and the accumulated GT strength for the decay of the  $3^+$  parent state in  $^{104}\text{Tc}$  to the calculated  $2^+$  and  $4^+$  daughter states in  $^{104}\text{Ru}$  (the  $3^+$  states do not have a significant contribution) is compared with TAGS results in Figure 4. The strong Gamow-Teller  $\beta$ -decay branches indicate essential contribution from the  $g_{9/2}^{\pi} g_{7/2}^{\nu}$ ,  $d_{5/2}^{\pi} d_{3/2}^{\nu}$  and  $d_{5/2}^{\pi} d_{5/2}^{\nu}$  matrix elements. Smaller contributions are obtained from  $p_{1/2}^{\pi} p_{3/2}^{\nu}$  and  $p_{3/2}^{\pi} p_{1/2}^{\nu}$  matrix elements. In the case of the decay of  $^{104}\text{Tc}$  to  $^{104}\text{Ru}$  the same matrix elements are relevant, but all of them are relatively small and the cancellations produce the final small strength for each Gamow-Teller contributing state. We have to mention that the best theoretical results based on other models are one order of magnitude outside the experimental data. The strong mixing of prolate and oblate projected configurations in the parent state as well as in the daughter states is responsible for the significant difference in the GT decays of  $^{102}\text{Tc}$  and  $^{104}\text{Tc}$ .

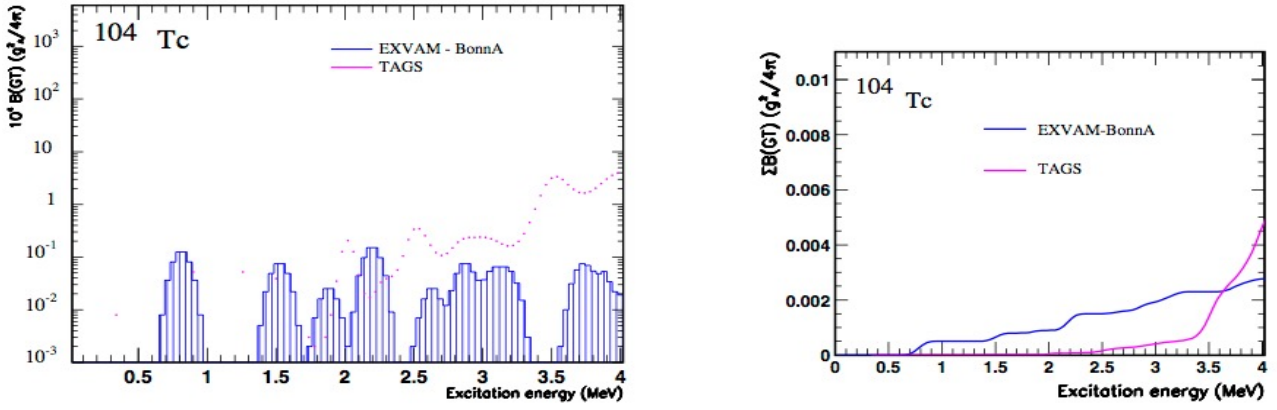


Fig. 4: The Gamow-Teller strength distribution and the corresponding accumulated strength for  $^{104}\text{Tc}$  obtained within the *complex* Excited Vampir model compared with TAGS results [4,5,6]

Also the deformation of the main configurations in the structure of the wave functions is smaller in the first case where the number of neutrons in the daughter nucleus has the critical value  $N = 58$  while in the second case the larger deformation is determined by  $N = 60$  in the  $^{104}\text{Ru}$  daughter nucleus. This results give support to our predictions concerning the role of the critical number of neutrons  $N=58$  for the structure and dynamics of neutron-rich nuclei with  $A\sim 100$  exemplified for  $^{96}\text{Sr}$  and  $^{98}\text{Zr}$  isotopes [5]. Our results are relevant predictions for the next experiments at FAIR, Germany, ISOLDE - CERN, Switzerland, RIKEN, Japan, and MSU, SUA.

### I. 3. Shape coexistence and shape evolution in the $N=58$ Kr isotope

The investigation of the neutron-rich nuclei in the  $A \approx 100$  mass region is receiving an increasing interest both theoretically and experimentally.

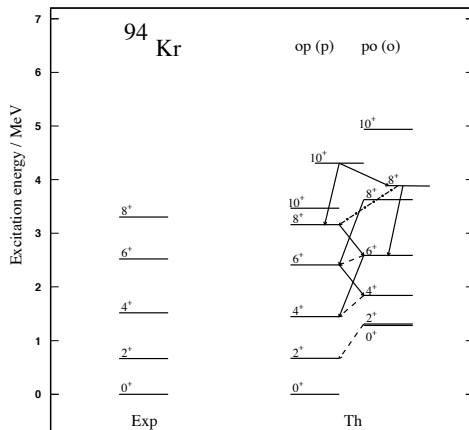


FIG. 5. The theoretical EXVAM spectrum of  $^{94}\text{Kr}$  is compared to the experimental data [7].

The oblate-prolate shape coexistence specific for each spin up to  $10^+$  and the evolution of the shape coexistence and mixing in the neutron-rich  $^{94}\text{Kr}$  isotope are studied within the *complex* Excited Vampir approach using a realistic effective interaction based on Bonn CD potential in a large model space. The influence of the shape mixing on the structure and dynamics of the lowest few positive parity states is discussed and comparison to the available data is presented.

The theoretical lowest bands of  $^{94}\text{Kr}$  are compared to the experimental spectrum in Figure 5. The good agreement with the available data gives support to our description of the structure of  $N=58$

isotopes of  $^{94}\text{Kr}$ ,  $^{96}\text{Sr}$ , and  $^{98}\text{Zr}$  based on shape coexistence and mixing that requires beyond-mean-field theoretical models for a realistic description of the coexistence phenomena revealed by the experimental data [6]. The labels of the bands indicate the prolate (p) or oblate (o) intrinsic quadrupole deformation for the dominant projected EXVAM configurations underlying the states of the corresponding bands. The states building the op(p)-band are characterised by strong prolate-oblate mixing at low spins and variable prolate mixing at intermediate spins.

The results concerning the oblate-prolate mixing in the structure of the wave functions for the lowest two states up to spin  $6^+$  and the lowest three states for spin  $8^+$  and  $10^+$  is illustrated in Table III. We indicate the contribution of the EXVAM configurations bringing at least 1% of the total amplitude.

Support for the mixing of configurations with different intrinsic deformations in the structure of the wave functions for the  $0^+$  states is offered by the strong  $\rho^2(E0)$  values for the transition from the second to the lowest  $0^+$  state. At intermediate spins specific aspects of shape coexistence and mixing have been identified. The present investigations will be continued and our *complex* Excited Vampir results will be compared with the new data obtained within the EXILL collaboration at ILL Grenoble, France.

Table III: The o-p mixing of the lowest calculated states.

$I[\hbar]$	o-mixing	p-mixing	$I[\hbar]$	o-mixing	p-mixing
$0_1^+$	62(4)%	32(2)%	$8_1^+$	1%	97(2)%
$0_2^+$	35(5)%	58(1)(1)%	$8_2^+$	92(3)(2)%	2(1)%
$2_1^+$	71(5)(1)%	22(1)%	$8_3^+$	3(2)%	87(7)(1)%
$2_2^+$	25%	74(1)%	$10_1^+$		80(19)(1)%
$4_1^+$	75(4)(1)%	19(1)%	$10_2^+$		63(15)(12)(9)%
$4_2^+$	20%	78%	$10_3^+$	94(4)(1)%	
$6_1^+$	40(3)(1)%	55(1)%			
$6_2^+$	58(1)%	40%			

#### I. 4. Structure of yrast states in $^{100}\text{Ru}$

We studied the evolution in structure with increasing spin in  $^{100}\text{Ru}$  within the *complex* Excited Vampir (EXVAM) variational model with symmetry projection before variation using a realistic

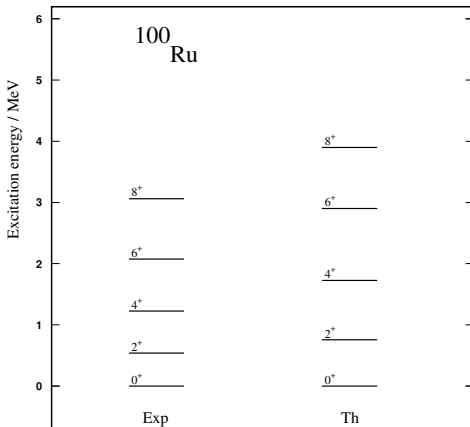


FIG. 6. The theoretical EXVAM spectrum of  $^{100}\text{Ru}$  is compared to the experimental data.

effective interaction based on Bonn CD potential in a large model space [8]. We investigated the lowest positive parity states up to spin  $8^+$  in  $^{100}\text{Ru}$  including in the Excited Vampir many-nucleon

bases up to 14 EXVAM configurations. The final solutions for each spin have been obtained diagonalizing the residual interaction between the considered Excited Vampir configurations.

Table IV: B(E2) values (in W.u.) connecting the calculated states (using different effective charges)

Transition	EXVAM	EXVAM
	( $e_p = 1.3, e_n = 0.3$ )	( $e_p = 1.4, e_n = 0.4$ )
$B(E2; 2_1^+ \rightarrow 0_1^+)$	20.5	26.7
$B(E2; 4_1^+ \rightarrow 2_1^+)$	34.2	44.4
$B(E2; 6_1^+ \rightarrow 4_1^+)$	37.5	48.6
$B(E2; 8_1^+ \rightarrow 6_1^+)$	32.4	42.4

The theoretical lowest band of  $^{100}\text{Ru}$  is compared to the experimental spectrum in Figure 6. The theoretical results on the B(E2) values for the yrast states are presented in Table IV compare nicely with the experimental data [8].

- 
- [1] A. Petrovici, Phys. Rev. C 85, 034337 (2012).
  - [2] A. Petrovici, K.W. Schmid, A. Faessler, AIP Conf. Proc. 1498, 38 (2012).
  - [3] A. Petrovici, K.W. Schmid, A. Faessler, J. Phys.: Conf. Ser. 413, 012007 (2013).
  - [4] D. Jordan, A. Petrovici et al, Phys. Rev. C 87, 044318 (2013).
  - [5] A. Petrovici, EPJ Web of Conf. 63, 01012 (2013).
  - [6] A. Petrovici, Hellenic Nuclear Physics Society, Proceedings HNPS2013, 59 (2014)
  - [7] A. Petrovici, invited talk at *EXILL Collaboration Meeting* - Bormio, Italy, February 22, 2016
  - [8] T. Konstantinopoulos, A. Petrovici et al., in preparation for Phys. Rev. C (2016).

**Relevant talks:**

1. *Shape coexistence, shape evolution and Gamow-Teller beta-decay of neutron-rich A~100 nuclei*, A. Petrovici, invited talk at Carpathian Summer School of Physics. Exotic Nuclei and Nuclear/ Particle Astrophysics (IV). From Nuclei to Stars, Sinaia, Romania, June 24 - July 7, 2012
2. *Exotic structure and decay of medium mass nuclei near the drip lines*, A. Petrovici, invited lecture at International Summer School for Advanced Studies on Dynamics of Open Nuclear Systems, Predeal, Romania, July 9-20, 2012.
3. *Shape coexistence in neutron-rich A~100 nuclei within beyond-mean-field approach*, A. Petrovici, overview talk at 2<sup>nd</sup> European Nuclear Physics Conference (EuNPC2012), Bucharest, Romania, September 17-21, 2012.
4. *Shape coexistence and shape evolution in neutron-rich A~100 nuclei*, A. Petrovici, talk at ISOLDE Workshop and Users meeting 2012, CERN-Geneva, Switzerland, December 17-19, 2012
5. *Shape evolution and Gamow-Teller beta-decay of neutron-rich A~100 nuclei within beyond-mean-field approach*, A. Petrovici, talk at Heavy Ion Accelerator Symposium on Fundamental and Applied Science (HIAS2013), Canberra, Australia, April 8-12, 2013
6. *Exotic structure and decay of medium mass nuclei near the drip lines*, A. Petrovici, invited talk at 22<sup>nd</sup> Symposium of the Hellenic Nuclear Physics Society (HNPS2013), University of Athens, Greece, May 31 - June 01, 2013.
7. *Coexistence phenomena in neutron-rich A~100 nuclei within beyond mean field approach*, A. Petrovici, invited talk at 3rd EXILL Workshop, Orsay, France, January 22-23, 2015
8. *Beyond-mean-field description of shape coexistence phenomena in neutron-rich A~100 nuclei*, A. Petrovici, invited talk at EXILL Collaboration Meeting - Bormio, Italy, February 22, 2016

## II. Coexistence phenomena in exotic proton-rich $A \sim 70$ nuclei within beyond-mean-field approach

### II.1. Isospin-symmetry-breaking and shape-coexistence effects in isovector triplets

#### II.1.1. Isospin-symmetry violation induced by Coulomb interaction

The properties of proton-rich nuclei in the  $A \sim 70$  mass region are not only relevant to nuclear structure, but are of high interest as micro-laboratory for high precision tests of the Standard Model. Shape coexistence and mixing, isospin mixing, competition between neutron-proton and like-nucleon pairing correlations are characteristic features of nuclei near the  $N=Z$  line in the  $A \sim 70$  mass region. We studied shape coexistence effects on Coulomb Energy Differences (CED) for  $A=66$  analogs [1] and the  $A=70$  isovector triplet [2] within the *complex* Excited Vampir model in a relatively large model space using a realistic effective interaction obtained from a nuclear matter G-matrix based on the Bonn A potential. Two-body correlations have been analyzed in the  $T=0$  and  $T=1$  channel relevant for the competition between the superallowed Fermi (F) and Gamow-Teller (GT)  $\beta$  decay. We investigated the possible shape coexistence phenomena in positive parity states up to spin  $8^+$  in  $^{66}\text{As}$  and  $^{66}\text{Ge}$  studying the influence of some particular two-nucleon correlations on the low energy spectra [1]. The theoretical results regarding the anomalous behaviour of CED with the spin evolution are in good agreement with the experimental data. It was revealed the essential effect of the mixing of differently deformed configurations on the anomalies in the behaviour of the CED for  $A \sim 70$  analogs. The comparison of our results with the available data are presented in Figure 1 [2].

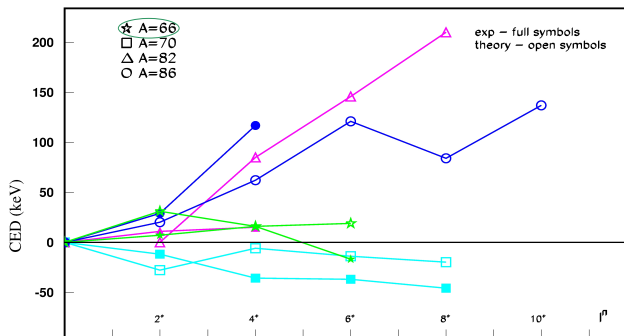


Fig.1: CED obtained within the *complex* Excited Vampir model compared to data [1].

The analysis of the wave functions in terms of nucleon pairs coupled to particular quantum numbers gives valuable information on the structure of the various states. In particular the competition between the different pairing modes in proton-rich nuclei could be revealed by the pair structure of the many-body wave functions.

We analyzed the pair structure of  $^{70}\text{Kr}$  and  $^{70}\text{Br}$ , members of the  $A = 70$  isovector triplet which manifest CED anomalies [2]. The motivation is connected with the possible competition of the superallowed Fermi and Gamow-Teller (GT)  $\beta$  decay of  $^{70}\text{Kr}$  to  $^{70}\text{Br}$  as a signature of the isoscalar proton-neutron pairing correlations. It is suggested in the literature that in medium mass nuclei an enhancement of the Gamow-Teller  $\beta$  decay of the ground state of an even-even  $Z = N + 2$  nucleus to the lowest  $I = 1^+$  state in the daughter odd-odd  $N = Z$  nucleus would be expected as a fingerprint of the neutron-proton  $T = 0$  condensate in the odd-odd system.

Using the same Hamiltonian as for the CED studies we constructed the lowest 8  $0^+$  states in  $^{70}\text{Kr}$  and the lowest 14  $0^+$  states and the lowest 10  $1^+$  states in  $^{70}\text{Br}$ . The lowest  $1^+$  states indicate a



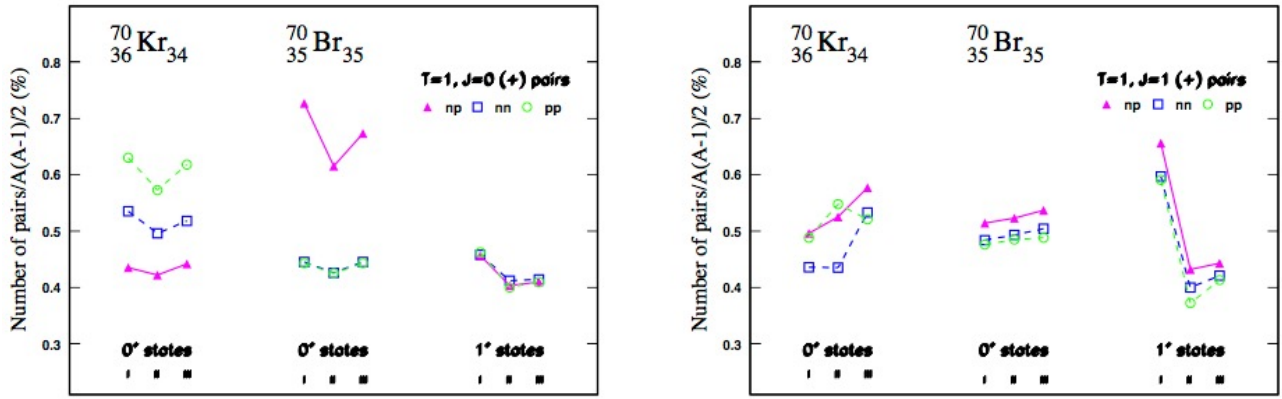


Fig.2. The number of nn, pp, and np pairs with  $T = 1$ ,  $J^\pi = 0^+$  and  $J^\pi = 1^+$  of the lowest  $0^+$  states in  $^{70}\text{Kr}$  and the lowest  $0^+$  and  $1^+$  states in  $^{70}\text{Br}$  given in percent of the sum rule [2].

completely different structure in terms of oblate-prolate mixing with respect to the  $0^+$  states. The EXVAM results for the Gamow-Teller  $\beta$  decay of the ground state of  $^{70}\text{Kr}$  indicate that the strength is distributed over many states, the GT branch to the lowest  $1^+$  state is very weak, while for the second and the third  $1^+$  states the strength is stronger.

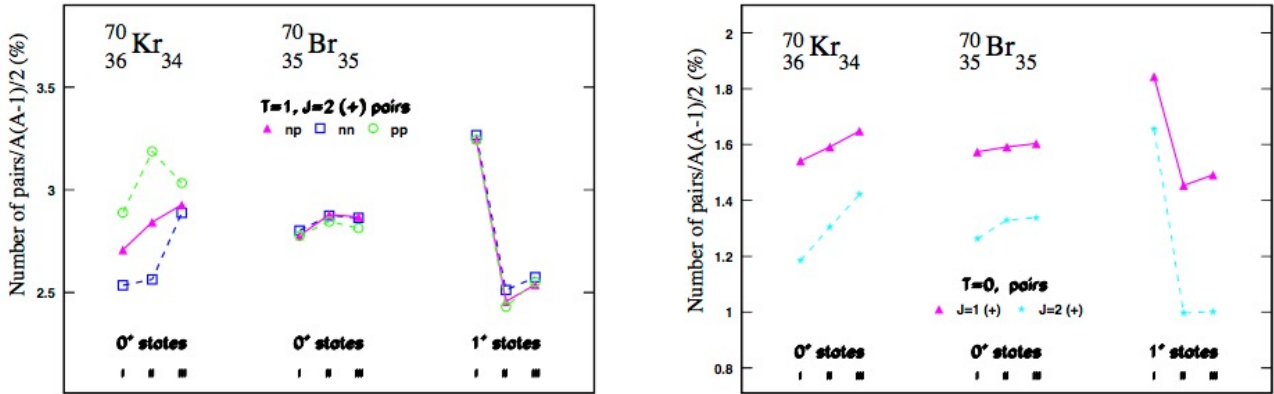


Fig.3. The same as in Fig.2 but for  $T = 1$ ,  $J^\pi = 2^+$  and  $T = 0$ ,  $J^\pi = 1^+$  and  $J^\pi = 2^+$ , respectively [2].

The pair structure analysis of the lowest three  $0^+$  states in the parent  $^{70}\text{Kr}$  and the daughter  $^{70}\text{Br}$  nucleus, involved in the superallowed Fermi beta decay, and the lowest three  $1^+$  states in  $^{70}\text{Br}$  relevant for the B(GT) analysis are illustrated in Figures 2 and 3. Contrary to the scenario proposed in the literature the maximum number of pairs has been obtained for the yrast  $1^+$  state characterised by negligible B(GT) strength. We have to mention that from the experimental study performed at GSI-Darmstadt on the Gamow-Teller  $\beta$  decay of the  $T = 1$   $0^+$  ground state of  $^{62}\text{Ge}$  into excited states of the odd-odd  $N = Z$   $^{62}\text{Ga}$  nucleus absence of the neutron-proton  $T = 0$  condensate was inferred from the weak B(GT) observed for the transition to the first  $1^+$  state.

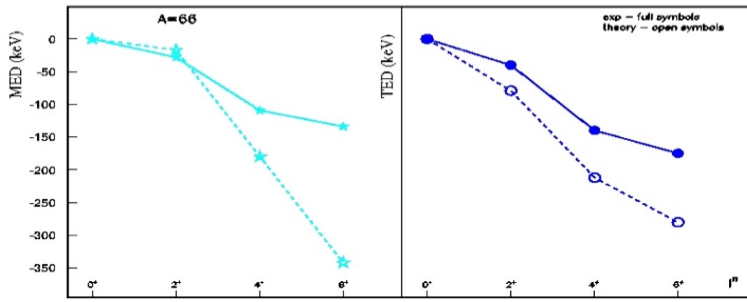


Fig.4. MED and TED for the A=66 isovector triplet [3]

Our analysis does not support the suggested scenario concerning the enhancement of the B(GT) strength in the Gamow-Teller  $\beta$  decay of the ground state of the even-even  $Z=N+2$  parent to the lowest  $1^+$  state in the odd-odd  $N=Z$   $^{70}\text{Br}$  daughter nucleus as a fingerprint for the neutron-proton  $T=0$  condensate.

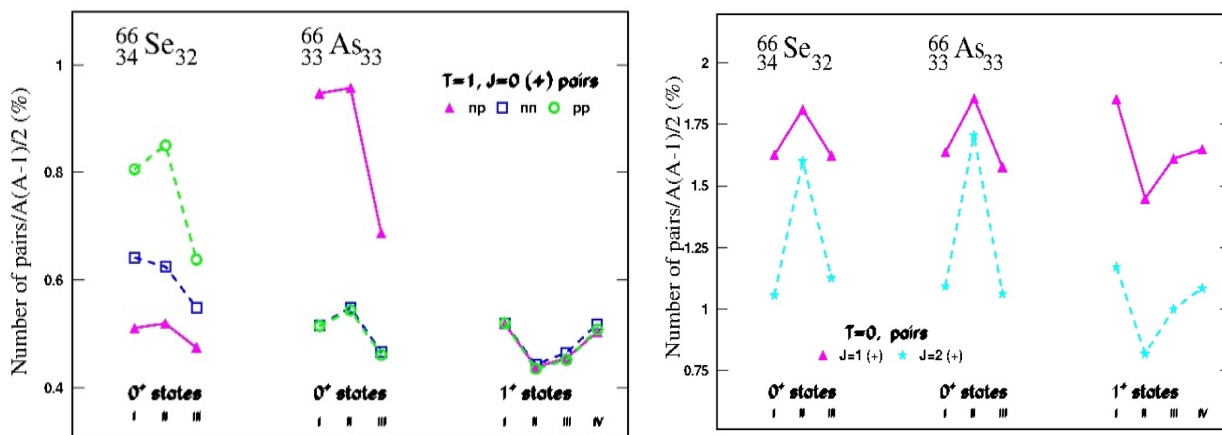


Fig. 5. The number of nn, pp, and np pairs with  $T=1, J^\pi=0^+$  and the number of np pairs with  $T=0, J^\pi=1^+$  and  $J^\pi=2^+$  of the lowest  $0^+$  in  $^{66}\text{Se}$  and the lowest  $0^+$  and  $1^+$  states in  $^{66}\text{As}$  in percent of the sum rule [3].

We studied shape coexistence effects on Mirror Energy Differences (MED) and Triplet Energy Differences (TED) in the A=66 isovector triplet. We also studied the two-body correlations in  $T=0$  and  $T=1$  channel relevant for the competition between the superallowed Fermi and Gamow-Teller (GT)  $\beta$  decay in the A=66 isovector triplet.

In  $^{66}\text{Se}$  we calculated the lowest positive parity states up to spin  $6^+$ . The results indicate that the projected prolate-deformed configurations in the intrinsic system dominate (more than 85%) the structure of the yrast states for each investigated spin. In Figure 4 we present the theoretical MED and TED for nuclei belonging to the A=66 isovector triplet predicted within the *complex* Excited Vampir model compared with available data including the recent results on  $^{66}\text{Se}$ . The theoretical results present the trend indicated by the experimental data.

We accomplished a pair structure analysis of  $^{66}\text{Se}$  and  $^{66}\text{As}$ , members of the A = 66 isovector triplet. The motivation is connected with the possible competition of the superallowed Fermi and Gamow-Teller (GT)  $\beta$  decay of  $^{66}\text{Se}$  to  $^{66}\text{As}$  as a signature of the isoscalar proton-neutron pairing correlations. In Figure 5 we present the results for the pair structure analysis of the lowest 3  $0^+$

states in  $^{66}\text{Se}$  and the lowest 3  $0^+$  states and the lowest 4  $1^+$  states in  $^{66}\text{As}$ . Relevant for the absence of the proposed scenario concerning the neutron-proton pairing condensation in the  $N=Z$  odd-odd systems is the plot presented in Figure 5 which indicates that the number of the neutron-proton pairs coupled to  $J^\pi = 1^+$ ,  $T=0$  is maximum for the lowest  $1^+$  state in  $^{66}\text{As}$  manifesting negligible Gamow-Teller strength.

We can conclude that we did not find an enhancement of the proton-neutron  $T=0$  pairing correlations for the Gamow-Teller contributing low-lying  $1^+$  states.

### II.1.2. Shape coexistence and isospin-related phenomena induced by Coulomb and strong force

The interplay between isospin-symmetry-breaking and shape-coexistence effects in  $A\sim 70$  analogs was self-consistently treated within the beyond-mean-field *complex* Excited Vampir variational model.

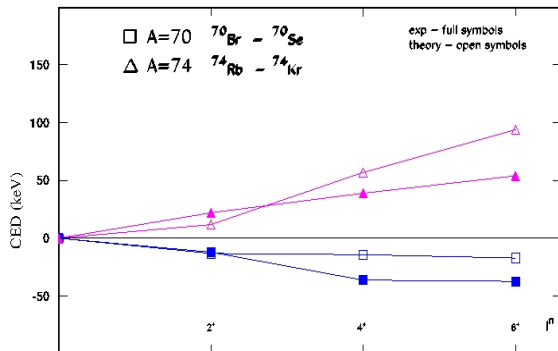


FIG. 6. Comparison of the *complex* excited VAMPIR results for CED to the experimental data [4].

We investigated the isospin-symmetry-breaking effects taking into account both the Coulomb interaction and the isospin-symmetry violation by the strong force as it is considered by the Bonn CD potential.

We illustrate the results on the effect of isospin mixing on CED, MED, TED, and TDE in the  $A=70$  and  $A=74$  isovector triplets investigating the  $0^+$ ,  $2^+$ ,  $4^+$ , and  $6^+$  states in these nuclei. Figure 6 presents the *complex* excited VAMPIR results on Coulomb energy differences for the  $^{70}\text{Br}$ - $^{70}\text{Se}$  and  $^{74}\text{Rb}$ - $^{74}\text{Kr}$  analogs compared with available data [4]. The trend manifested in the data is reproduced by the EXVAM results for the  $A = 74$  pair of nuclei as well as the anomalous behaviour revealed for the  $^{70}\text{Br}$ - $^{70}\text{Se}$  case.

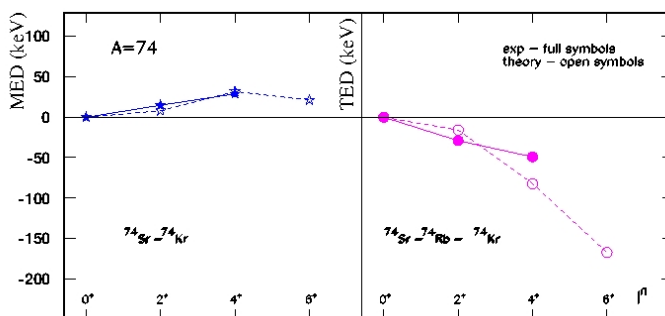


FIG. 7. The *complex* Excited VAMPIR results for MED and TED in the  $A=74$  isovector triplet compared to data [5].

Figure 7 illustrates the *complex* Excited VAMPIR predictions on mirror energy differences and triplet energy differences for the  $A = 74$  isovector triplet. MED manifest a positive trend, while TED indicate a negative trend, in agreement with the recent experimental available results [5]. These results represent the first beyond-mean-field treatment based on an effective two-body interaction constructed from the nuclear matter G matrix starting from the charge-dependent Bonn CD potential able to describe self-consistently the isospin-symmetry-breaking effects in a region dominated by shape coexistence and mixing.

## II.2. Shape coexistence effects on terrestrial and stellar weak interaction rates

### II.2.1. $^{68}\text{Se}$ and $^{72}\text{Kr}$ rp-process waiting points

Self-consistent microscopic approaches capable of describing the experimentally accessible properties of nuclei are needed to predict nuclear characteristics beyond the experimental reach required by nuclear astrophysics. In particular, properties of exotic nuclei difficult to explore experimentally are relevant for astrophysical scenarios of explosive phenomena like X-ray bursts. This is the case of nuclei in the  $A \sim 70$  mass region involved in the nucleosynthesis rapid proton-capture (rp) process.

The coexistence phenomena dominating the structure and dynamics of medium mass proton-rich nuclei have been intensively investigated within the *complex* Excited Vampir approach and many predictions that emerged have been experimentally confirmed. The present study is the first attempt at a completely self-consistent calculation of the stellar weak interaction rates for  $^{68}\text{Se}$  and  $^{72}\text{Kr}$  waiting-point nuclei at densities  $\rho = 10^4 - 10^7 \text{ g/cm}^3$  and temperatures  $T = 10^8 - 10^{10} \text{ K}$  using the *complex* Excited Vampir model.

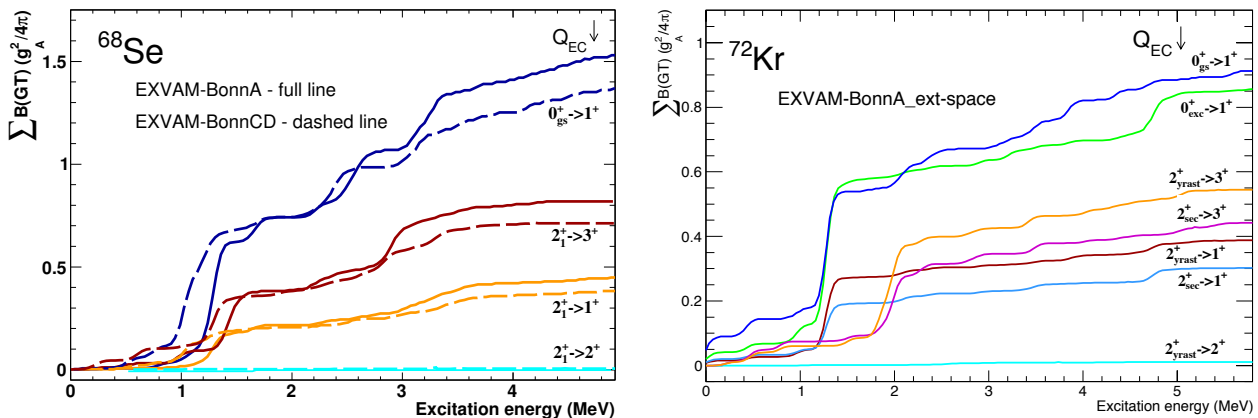


Fig. 8: Gamow-Teller accumulated strengths for the decay of low-lying  $0^+$  and  $2^+$  states in  $^{68}\text{Se}$  (left) and  $^{72}\text{Kr}$  (right) obtained within *complex* Excited Vampir model [6,7].

We extended the previous studies on Gamow-Teller decay of  $^{68}\text{Se}$  using the standard model space and the effective interactions obtained starting from Bonn A and Bonn CD potential [6]. The mixing of the differently deformed configurations in the intrinsic system in the structure of the yrast  $2^+$  state in  $^{68}\text{Se}$  indicates 60% (41%) oblate content for Bonn A (Bonn CD) potential. Consequently, the spectroscopic quadrupole moment is changing from  $3.5 \text{ efm}^2$  for Bonn A to  $-7.1 \text{ efm}^2$  for Bonn CD (extracharge of 0.3 e is used). The characteristics of the projected Excited Vampir

configurations are not significantly modified by replacing Bonn A with Bonn CD potential, but their mixing in the structure of the final wave functions is changed. In Figure 8 (left) are compared the accumulated Gamow-Teller strengths obtained using Bonn A and Bonn CD potential for the decay of the ground state and yrast  $2^+$  state in  $^{68}\text{Se}$  to EXVAM  $1^+$ ,  $2^+$ , and  $3^+$  states in  $^{68}\text{As}$ . The measured half-life of  $^{68}\text{Se}$  is 35.5(7) s and the beta window is  $Q_{\text{EC}} = 4730(310)$  keV. The EXVAM result for the terrestrial half-life is 48.8 (33.5) s using Bonn A (Bonn CD) potential.

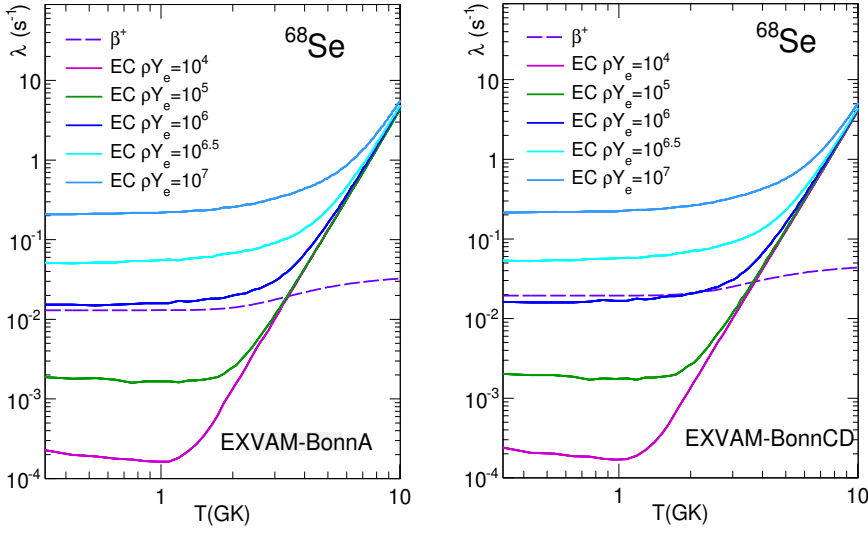


Fig. 9. Decay rates ( $\text{s}^{-1}$ ) for the ground state and yrast  $2^+$  state in  $^{68}\text{Se}$  decomposed into the corresponding  $\beta^+$  and electron capture components for selected densities  $\rho Y_e$  ( $\text{mol}/\text{cm}^3$ ) as a function of temperature  $T$  (GK) obtained using the Bonn A (left) and Bonn CD (right) potential.

For the  $^{72}\text{Kr}$  waiting point nucleus we extended the previous investigations calculating the Gamow-Teller distribution strengths for the decay of the ground state, the lowest excited  $0^+$ , the yrast and second  $2^+$  state in an extended model space using the Bonn A potential [6].

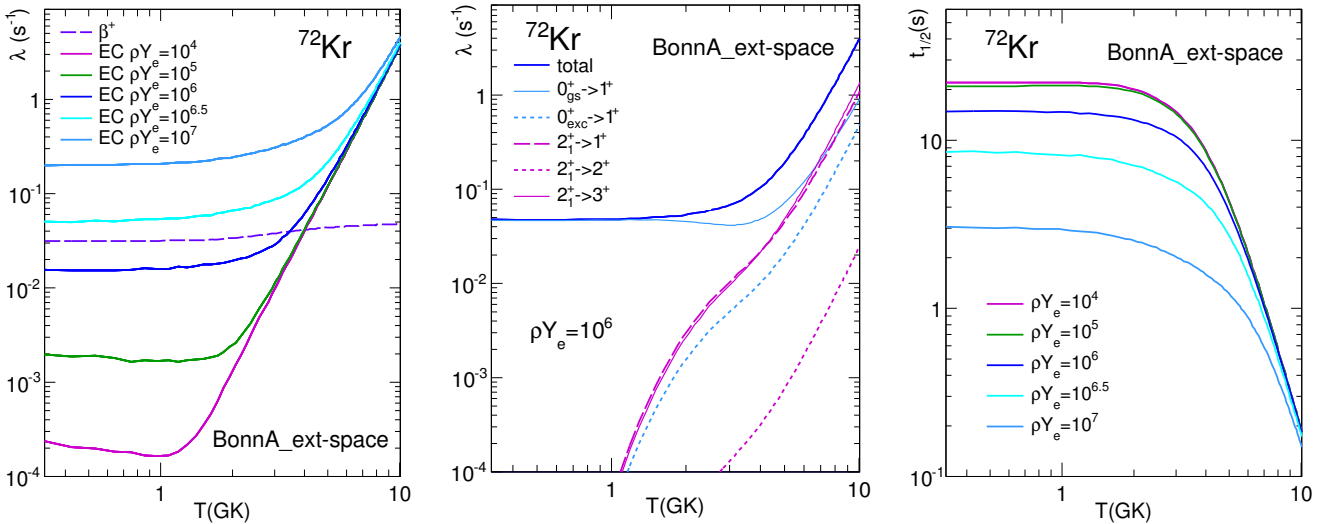


Fig. 10: Decay rates ( $\text{s}^{-1}$ ) for the ground state and yrast  $2^+$  state in  $^{72}\text{Kr}$  for selected densities  $\rho Y_e$  ( $\text{mol}/\text{cm}^3$ ) as a function of temperature  $T$  (GK) decomposed into  $\beta^+$  and electron capture components (left) and into contributions of different parents states (middle) and corresponding half-lives (s) (right) [6].

In Figure 8 (right) we present the EXVAM Gamow-Teller accumulated strengths for the decay of the investigated parent states in  $^{72}\text{Kr}$ . In  $^{68}\text{Se}$  the theoretical results are obtained using an effective interaction based on Bonn A/Bonn CD potential in the standard model space while in the  $^{72}\text{Kr}$  results are calculated in an extended model space using Bonn A potential [6]. The experimental value of the half-life for the decay of the ground state of  $^{72}\text{Kr}$  is 17.1(2) s, whereas the Excited Vampir result is 20.8(20.7) s for the Bonn A potential in the standard (extended) model space and 18.9 s in the standard model space for the Bonn CD potential.

The general formalism to calculate weak interaction rates for a stellar environment has been introduced by Fuller et al. in 1980. Since in the ranges of densities and temperatures relevant for the rp process the stellar beta decay and continuum electron capture are sensitive to the Gamow-Teller strength distributions a realistic treatment of the shape coexistence and mixing dominating the structure of the low-lying states in parent nuclei and the corresponding states in daughter nuclei is required.

For the rp-process waiting point nucleus  $^{68}\text{Se}$  we investigated the influence of shape coexistence and mixing on stellar weak interaction rates taking into account the thermally populated yrast  $2^+$  state situated at 854 keV excitation energy.

In Figure 9 is illustrated the effect of the changes induced in the shape mixing replacing Bonn A by Bonn CD potential on the evolution of the decay rates as a function of temperature for selected densities  $\rho Y_e$ . The decay rates for the ground state and yrast  $2^+$  state of  $^{68}\text{Se}$  are decomposed into the corresponding  $\beta^+$  and continuum electron capture components. For the rp-process typical density  $\rho Y_e = 10^6 \text{ mol/cm}^3$  one can observe that for the results obtained using Bonn CD potential the electron capture overcomes the  $\beta^+$  component only at temperatures larger than 2 GK.

The induced differences in the oblate-prolate mixing for the parent as well as daughter states are responsible for a variation of 24% for the half-life obtained at  $T = 1.5 \text{ GK}$  and  $\rho Y_e = 10^6 \text{ mol/cm}^3$ .

The investigation of the rp-process waiting point nucleus  $^{72}\text{Kr}$  included the thermally populated first excited  $0^+$  state and yrast  $2^+$  state situated at 671 keV and 710 keV, respectively, calculated using different model spaces (standard and extended) and effective interactions obtained starting from Bonn A and Bonn CD potential.

In Figure 10 are presented the total decay rates decomposed into the corresponding  $\beta^+$  and electron capture components and into the contribution of different parent states, and the half-lives for selected densities  $\rho Y_e$  as a function of temperature obtained using Bonn A potential in the extended model space for  $^{72}\text{Kr}$  nucleus.

These results represent the first beyond-mean-field treatment based on realistic effective interactions in rather large model spaces able to describe self-consistently the effect of shape coexistence and mixing on the stellar weak interaction rates for  $A \sim 70$  rp-process waiting point nuclei manifesting variable shape mixing with increasing spin and excitation energy [6]. The realistic description of the shape coexistence and mixing dominating the structure of the  $^{68}\text{Se}$  and  $^{72}\text{Kr}$  waiting points as well as the daughter  $^{68}\text{As}$  and  $^{72}\text{Br}$  nuclei, respectively, reveal significant effects on the stellar decay rates at the rp-process typical conditions of temperature and densities.

## II.2.2. The $Z=N+2$ $^{70}\text{Kr}$ and $^{74}\text{Sr}$ isotopes

We studied the effects of shape mixing on the weak interaction rates for the  $Z=N+2$   $^{70}\text{Kr}$  and  $^{74}\text{Sr}$  isotopes describing the low-lying  $0^+$  and  $2^+$  states in the parent nuclei and the corresponding daughter  $0^+$ ,  $1^+$ ,  $2^+$ , and  $3^+$  states in  $^{70}\text{Br}$  and  $^{74}\text{Rb}$ , respectively [8], within the *complex* Excited Vampir model based on the effective interaction obtained from the charge-dependent Bonn CD potential and the model space previously used to investigate the isospin-related phenomena in the isovector triplets with  $A=70$  and  $A=74$  [4].

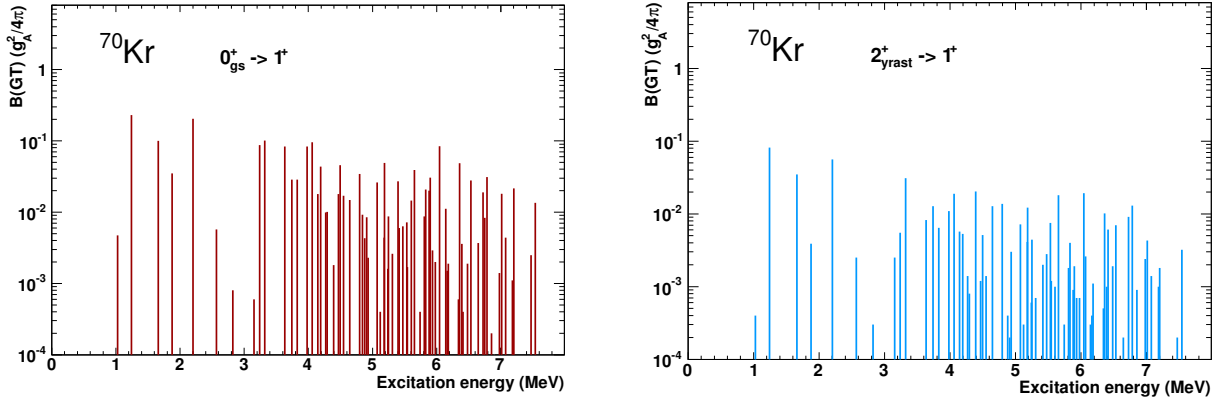


FIG. 11. Gamow-Teller strength distributions for the decay of the ground state and yrast  $2^+$  in  $^{70}\text{Kr}$  to  $1^+$  states in  $^{70}\text{Br}$  obtained within the *complex* Excited Vampir model [7].

Our study was the first attempt at a completely self-consistent calculation of the terrestrial and stellar weak interaction rates for  $^{70}\text{Kr}$  and  $^{74}\text{Sr}$  at densities  $\rho = 10^4 - 10^7 \text{g/cm}^3$  and temperatures  $T = 10^8 - 10^{10} \text{K}$  using the *complex* Excited Vampir approach [8].

For the investigation of the Fermi and Gamow-Teller  $\beta$ -decay properties of the lowest two  $0^+$  and

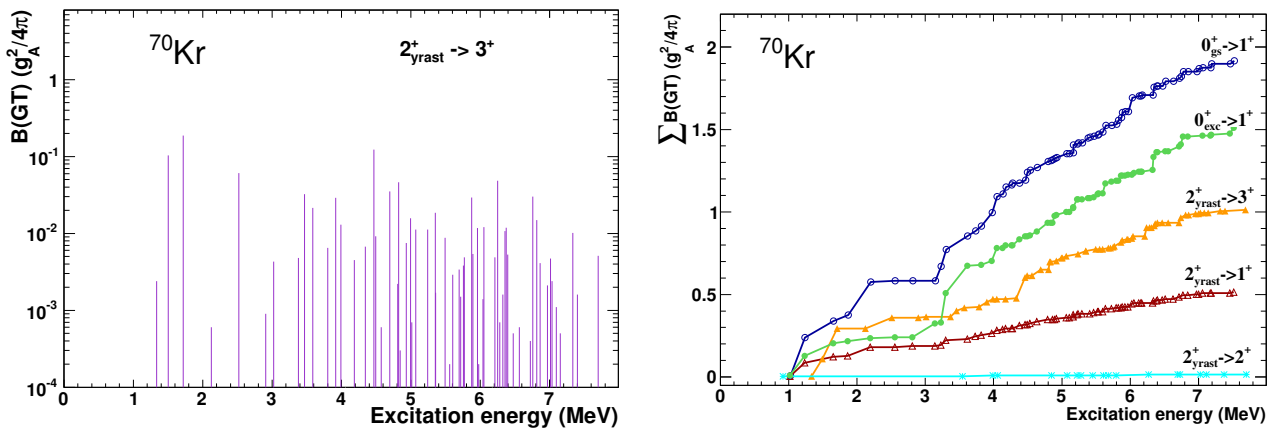


Fig. 12. The same as in Fig.11, but for the decay to  $3^+$  states in  $^{70}\text{Br}$ .

Fig.13. GT accumulated strengths for the decay of low-lying  $0^+$  and  $2^+$  states in  $^{70}\text{Kr}$ .

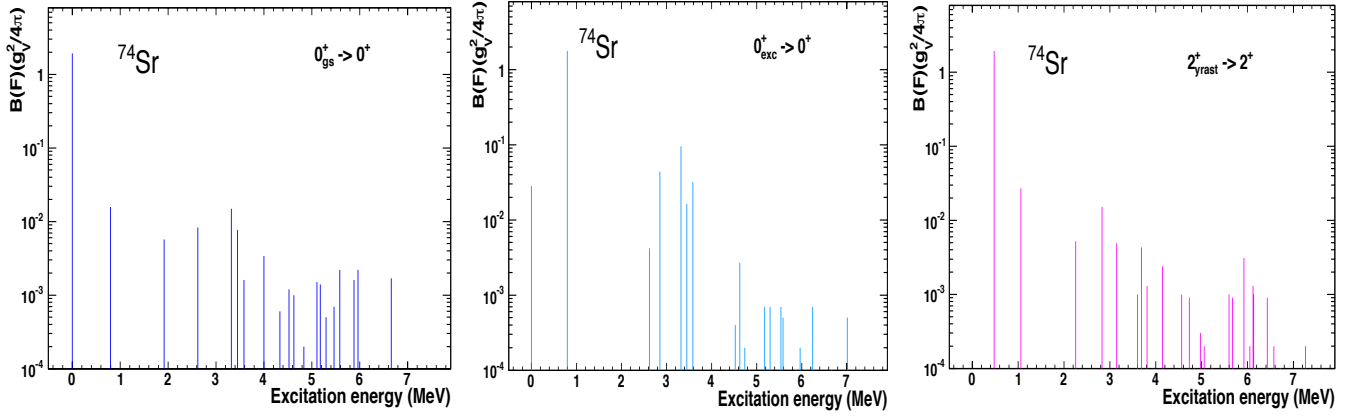


FIG. 14. Fermi strength distributions for the decay of low-lying  $0^+$  and  $2^+$  states in  $^{74}\text{Sr}$  [5].

$2^+$  states in  $^{70}\text{Kr}$  we extended the calculations presented in [4] to the daughter states in the  $^{70}\text{Br}$  nucleus [5,8]. The *complex* Excited Vampir results on the Gamow-Teller strength distributions for decay of the  $0^+$  ground state and yrast  $2^+$  in  $^{70}\text{Kr}$  to the  $1^+$  and  $3^+$  states in  $^{70}\text{Br}$  are presented in Figure 11 and Figure 12, respectively. The GT accumulated strengths presented in Figure 13 for the decay of the ground state, first excited  $0^+$ , and yrast  $2^+$  state in  $^{70}\text{Kr}$  to the daughter states in  $^{70}\text{Br}$  indicate stronger strength from the ground state decay with respect to that from the first excited  $0^+$  state and larger contributions from the decay of the yrast  $2^+$  state to the daughter  $3^+$  states than the ones to the  $1^+$  states. Fermi strength distributions have been realistically investigated for low-lying  $0^+$  and  $2^+$  states in  $^{70}\text{Kr}$  and  $^{74}\text{Sr}$  (results are illustrated in Figure 14 for  $^{74}\text{Sr}$ ).

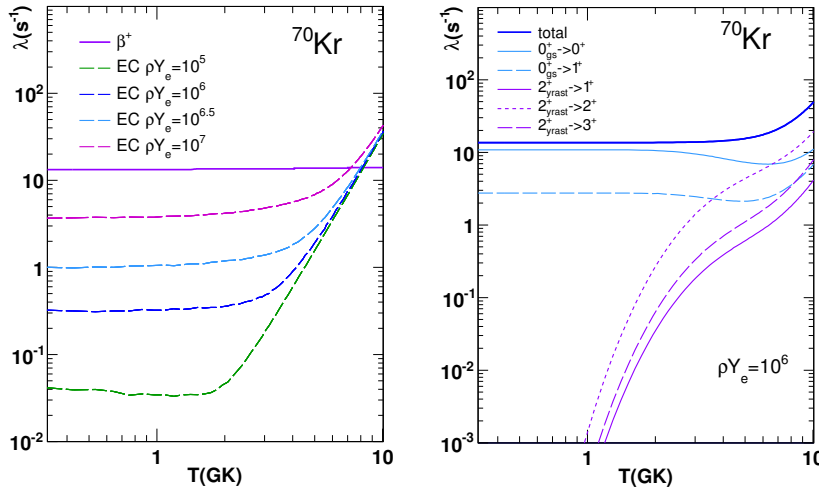


FIG. 15. Fermi and Gamow-Teller decay rates ( $\text{s}^{-1}$ ) for the ground state and yrast  $2^+$  state in  $^{70}\text{Kr}$  decomposed into the corresponding  $\beta^+$  and electron capture components for selected densities  $\rho Y_e$  ( $\text{mol}/\text{cm}^3$ ) (left) and total decay rates for rp-process peak density (right) as a function of temperature  $T$  (GK) [8].

The *complex* Excited Vampir result for the Gamow-Teller half-life of the ground state of  $^{70}\text{Kr}$  is 258 ms and for the Fermi decay is 63 ms. Consequently, the theoretical half-life of the ground state amounts to 51 ms in good agreement with the available experimental adopted value of 52(17) ms.



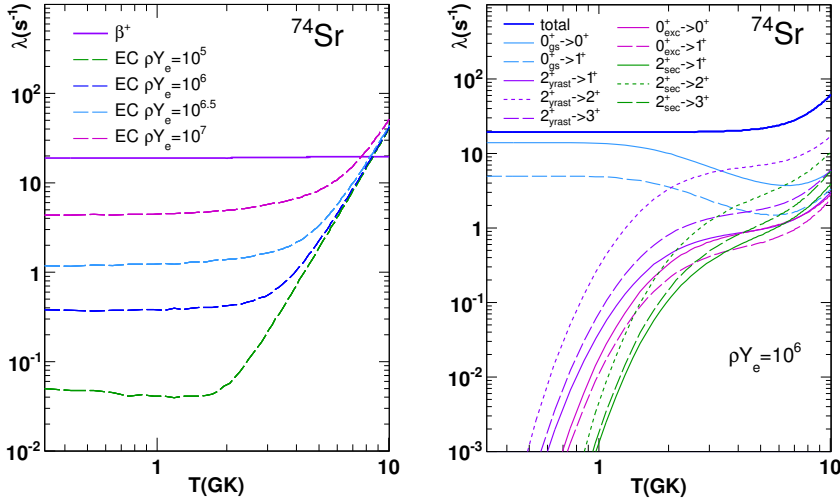


FIG. 16 The same as in Fig. 15, but for  $^{74}\text{Sr}$  nucleus [8].

For the  $Z=N+2$  nucleus  $^{70}\text{Kr}$  we investigated the influence of the yrast  $2^+$  state decay on the effective half-life given the predicted high excitation energy of the first excited  $0^+$  and the second  $2^+$  states.

As it is illustrated in Figure 15 (left) the contribution of the electron capture is very small at the temperatures (1 – 3GK) and densities ( $10^6 - 10^7\text{g/cm}^3$ ) characteristic for the rp-process astrophysical environment. The total decay rates for  $^{70}\text{Kr}$  at the rp-process peak density as a function of temperature are presented in Fig. 15 (right) decomposed into the contributions from the ground state and yrast  $2^+$  state.

Extended investigations have been accomplished for the  $Z=N+2$   $^{74}\text{Sr}$  nucleus. Fermi and Gamow-Teller decay rates for the low-lying  $0^+$  and  $2^+$  states in  $^{74}\text{Sr}$  are presented in Figure 16.

The present report represent the first beyond-mean-field treatment based on an effective two-body interaction constructed from the nuclear matter G-matrix starting from the charge dependent Bonn CD potential able to describe self-consistently the allowed Fermi and Gamow-Teller  $\beta$ -decay [7,8] as well as the effect of shape coexistence on isospin-related phenomena in the  $A=70$  and  $A=74$  isovector triplets [4,5] in a region dominated by shape coexistence and mixing. Furthermore, we use a model space adequate for the description of proton-rich nuclei in the  $A\sim 70$  mass region which is not yet numerically feasible for the large-scale shell-model calculations. Experimental strength distributions and spectroscopic quadrupole moments for the parent and daughter states could test our predictions on the influence of shape mixing on weak interaction rates.

- 
- [1] G. de Angelis, A. Petrovici et al, Phys. Rev. C 85, 034320 (2012).
  - [2] A. Petrovici, Rom. J. Phys. 58, 1120 (2013).
  - [3] A. Petrovici and O. Andrei, AIP Conf. Proc. 1645, 21 (2015)
  - [4] A. Petrovici, Phys. Rev. C 91, 014302 (2015)
  - [5] A. Petrovici, J. Phys. Conf. Ser. 724, 012038 (2016)
  - [6] A. Petrovici and O. Andrei, Eur. Phys. J. A 51, 133 (2015)
  - [7] A. Petrovici and O. Andrei, will appear in AIP Conf. Proc. (2016)
  - [8] A. Petrovici and O. Andrei, Phys. Rev. C 92, 064305 (2015)

**Relevant talks:**

1. *Nucleon-nucleon correlations in exotic nuclei*, A. Petrovici, invited talk at Structure and Reactions for Exotic Nuclei (SARFEN) Meeting, Trento, Italy, March 26-27, 2012
2. *Exotic structure and decay of medium mass nuclei near the drip lines*, A. Petrovici, invited lecture at International Summer School for Advanced Studies on Dynamics of Open Nuclear Systems, Predeal, Romania, July 9-20, 2012.
3. *Exotic structure and decay of medium mass nuclei near the drip lines*, A. Petrovici, invited talk at 22<sup>nd</sup> Symposium of the Hellenic Nuclear Physics Society (HNPS2013), University of Athens, Greece, May 31 - June 01, 2013.
4. *Exotic structure and decay of medium mass nuclei near the drip lines within beyond-mean-field approach*, A. Petrovici, invited talk at Nuclear Structure Physics with Advanced Gamma-Detector Arrays (NSP13), Padova, Italy, June 10-12, 2013.
5. *Shape-coexistence effects on the structure and dynamics of  $A\sim 70$  proton-rich nuclei within beyond-mean-field approach*, A. Petrovici, invited talk at From nuclear structure to particle-transfer reactions and back, ECT\*, Trento, Italy, November 4-8, 2013.
6. *Exotic structure and decay within beyond-mean-field approach*, A. Petrovici, invited talk at TAS Collaboration Workshop: Status and Perspectives, Valencia, Spain, June 26-28, 2014.
7. *Isospin-symmetry-breaking effects in  $A\sim 70$  nuclei within beyond-mean-field approach*, A. Petrovici, invited talk at the Carpathian Summer School of Physics 2014, Sinaia, Romania, July 13-26, 2014.
8. *Isospin-symmetry-breaking and shape-coexistence effects in  $A\sim 70$  analogs within beyond-mean-field approach*, A. Petrovici, invited talk at From nuclear structure to particle-transfer reactions and back II, ECT\*, Trento, Italy, November 10-14, 2014
9. *Isospin-symmetry-breaking and shape-coexistence effects on structure and dynamics of medium mass nuclei*, A. Petrovici, talk at LIA Romania-France workshop, Magurele, Romania, December 3-5, 2014
10. *Isospin-symmetry breaking and shape coexistence in  $A\sim 70$  analogs*, A. Petrovici, invited talk at XXI International School on Nuclear Physics and Applications & International Symposium on Exotic Nuclei (2015), Varna, Bulgaria, September 06-12, 2015
11. *Realistic description of isospin-related phenomena in  $A\sim 70$  analogs*, A. Petrovici, seminar at CSNSM, Orsay, Paris, November 13, 2015
12. *Stellar weak interaction rates and shape coexistence for  $A\sim 70$  proton-rich nuclei within beyond-mean-field approach*, A. Petrovici, invited talk at III<sup>rd</sup> Topical Workshop on Modern Aspects in Nuclear Structure: The Many Facets of Nuclear Structure, Bormio, Italy, February 22-28, 2016
13. *From isospin mixing to stellar weak interaction rates within beyond-mean-field approach*, A. Petrovici, invited talk at NUSTAR Annual Meeting 2016, GSI Darmstadt, Germany, February 29 - March 4, 2016
14. *Shape coexistence effects on isospin-symmetry breaking and beta decay of proton-rich  $A\sim 70$  nuclei*, A. Petrovici, talk at NUSPIN 2016 Workshop of the Nuclear Spectroscopy Instrumentation Network and AGATA Physics Workshop, Venice, Italy, June 27- July 1, 2016
15. *Shape coexistence effects on stellar weak interaction rates of proton-rich nuclei within beyond-mean-field approach*, A. Petrovici, invited talk at Carpathian Summer School of Physics 2016, Sinaia, Romania, June 26 - July 9, 2016
16. *From Isospin-Related Phenomena to Stellar Weak Processes within Beyond - Mean - Field Approach*, A. Petrovici, talk at Nuclear Structure 2016, Knoxville, Tennessee, USA, July 24-29, 2016.

## Summary

Within the present project we addressed essential questions concerning the structure and dynamics of exotic nuclei and tests of fundamental interactions and symmetries. A comprehensive description of coexistence phenomena in exotic proton-rich nuclei in the  $A \sim 70$  mass region and exotic neutron-rich nuclei in the  $A \sim 100$  region was obtained in the frame of the beyond-mean-field variational approaches with symmetry projection before variation belonging to the *complex* Vampir model family. For a realistic description of the investigated nuclei we involved realistic effective interactions obtained by systematic studies of medium mass nuclei with exotic  $Z/N$  ratios in large model spaces. Realistic predictions on weak interaction rates under terrestrial and stellar environment for nuclei dominated by shape coexistence with relevance for nucleosynthesis and significance for astrophysical scenarios concerning the rp-process path have emerged.

In conclusion, the results obtained within the project PN-II-ID-PCE-2011-3-0153, unique in the literature, correspond to the project objectives.

Project leader,

Alexandrina Petrovici